In silico Studies Combining QSAR Models, DFT-based Reactivity Descriptors and Docking Simulations of Phthalimide Congeners with Hypolipidemic Activity

Camila da Câmara Lopes [a], Maria Angélica Bonfim Oliveira [a], Regiane de Cássia Maritan Ugulino de Araújo [b], and Boaz Galdino de Oliveira [ID] [a]

In this current study, a selected group of physicochemical descriptors extracted from the formalism of the density functional theory were used for modeling a series of phthalimide congeners with tested hypolipidemic activity once. Based on unsupervised pattern recognition of HCA and PCA followed by the PLS regressions, the final content may be considered trustful for predicting the biological activity due to the results of r^2_{cal} = 0.937, r^2_{cv} = 0.591 and r^2_{test} = 0.85. Moreover, the molecular modeling was performed through the docking protocol for predicting the ligand pose on the HMG-CoA reductase. The protocols of the AutoDock Tools and AutoDock Vina were used for determining the interaction scores (ΔG) and inhibition constants (K_i). Among all congeners studied, the docking results pointed out a potential compound. By taking into account the widely known top selling drugs, and just as is well-known that atorvastatin is one of them due its capability to lower the cholesterol levels, the structure of this drug was subjected to a docking study in order to guide us to a better understanding of the results available here.

Graphical abstract
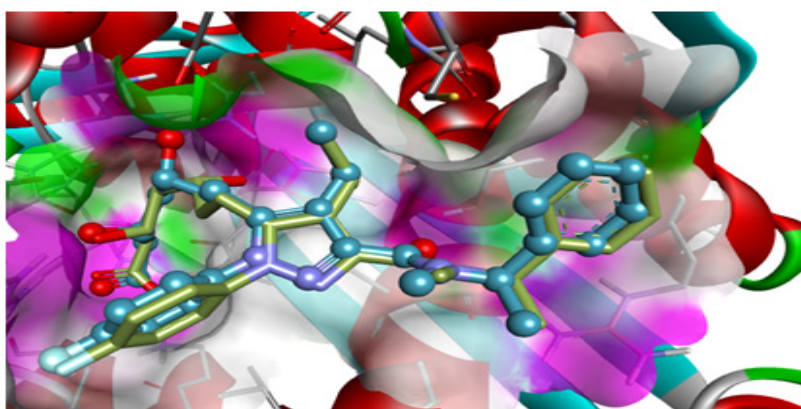
1. Introduction

According to reports of the World Health Organization (WHO) [1], one of the most important vectors of clinical mortality concerns to the cardiovascular diseases, which in 2019 reached the mark of 17.9 million of patients all over the globe [2-3]. In view of this, continuously many governmental health programs are elaborated in order to confront this

[a] Centro das Ciências Exatas e das Tecnologias, Universidade Federal do Oeste da Bahia, Campus Reitor Edgard Santos, 47805-000 Barreiras, BA, Brazil. [b] Departamento de Química – Centro das Ciências Exatas e da Natureza, Universidade Federal da Paraíba, 58051-900 João Pessoa, PB, Brazil. *Corresponding author. E-mail: **boazgaldino@gmail.com**

problem [4], mainly focusing on the combat of risk factors, such as high blood pressure and lipid levels in the human organism beyond the allowable limit [5]. In the clinical treatment [6-7], the drug administration is still one of the most efficient methods to retard or stop the progress of the cardiovascular diseases [8], by which it must be cited the statin [9] as one faithful representative of the drugs highly efficient [10], and ideally followed by several candidates to compounds that behave very promising in this regard [11-13]. Meantime, besides the statin (Figure 1.A), the phthalimides or imides as derivatives of the phthalic acid composed by two carbonyl groups linked by a secondary amine as well as the N-substituted phthalimides (Figure 1.B), all these ones are also important classes of compounds [14], which, under experimental conditions, they are obtained by accessible synthetic routes and highly efficient in lipid-lowering therapies [15-16]. In this context, the reducing values in percentage of the cholesterol (C_{16}) and triglyceride (T_{16}) [17-19] have

received a preliminary statistical treatment to find the negative logarithm results (-Log), which are also organized in Table 1.
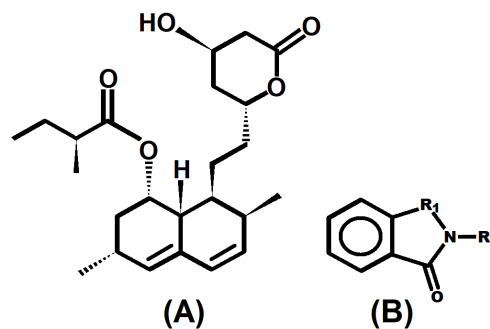
Fig. 1. Structure of the statin (**A**) and phthalimide derivatives (**B**). Substituent groups are presented in Table 1.

Table 1. Substituent groups R_1 and R_2 in the phthalimide congeners and their respective percentage values of cholesterol and triglyceride after 14-16 days of treatment (20mg/kg/day) in mice.

Congeners	Substituent groups		Biological activities			
	R_1	R_2	C_{16}	pC_{16}	$T_{14/16}$	$pT_{14/16}$
1[a]	CO	H	57 ± 7	-1.75	44 ± 8 (14 days)	-1.64
2[a]	CO	n-C_4H_9	54 ± 6	-1.73	82 ± 10 (14 days)	-1.91
3[b]	CNH	H	56 ± 4	-1.74	59 ± 5 (16 days)	-1.77
4[a]	CH_2	n-C_4H_9	62 ± 7	-1.79	80 ± 8 (14 days)	-1.90
5[c]	NH	H	80 ± 6	-1.90	75 ± 6 (16 days)	-1.87
6[c]	NH	CH_3	69 ± 5	-1.83	72 ± 5 (16 days)	-1.85
7[c]	NH	C_2H_5	71 ± 6	-1.85	71 ± 6 (16 days)	-1.85
8[c]	NH	n-C_3H_7	68 ± 5	-1.83	77 ± 6 (16 days)	-1.88
9[c]	NH	n-C_5H_{11}	73 ± 6	-1.86	77 ± 6 (16 days)	-1.88
10[d]	CO	ϕ-m-C_2H_5	82 ± 10	-1.91	95 ± 4 (14 days)	-1.97
11[d]	CO	ϕ-p-C_2H_5	89 ± 60	-1.94	96 ± 4 (14 days)	-1.98
12[a]	CO	n-C_5H_{11}	58 ± 7	-1.76	75 ± 6 (14 days)	-1.87
13[a]	SO_2	CH_2COCH_3	52 ± 5	-1.71	66 ± 8 (14 days)	-1.81
14[a]	SO_2	C_2H_4COCH3	62 ± 6	-1.79	51 ± 7 (14 days)	-1.70
15[a]	SO_2	C_2H_4COOH	47 ± 5	-1.67	67 ± 7 (14 days)	-1.82
16[a]	SO_2	C_3H_6COOH	73 ± 6	-1.86	48 ± 8 (14 days)	-1.68
17[a]	SO_2	C_4H_8COOH	68 ± 8	-1.83	44 ± 6 (14 days)	-1.64
18[a]	CO	CH_2COCH_3	67 ± 12	-1.82	48 ± 10 (14 days)	-1.68

Experimental values of C_{16} and T_{16} are given in %. [a]: Ref. [20]; [b]: Ref. [21]; [c]: Ref. [22] and [d]: Ref. [23].

Bearing in mind what is known, regardless if at light of industrial procedures or academic researches [24-25], many years of high-level research supported by huge financial investments summarize what we know as being indispensable requirements to the development of a pharmacological drug [26-27]. In order to improve these two onerous factors, some time ago the use of computational tools has provided a cost reduction up to 50% for producing any kind of pharmaceutical drug [28-30]. This is known as Computer-Aided Drug Design (CADD) [31], wherein the molecular modeling with direct dependency of the biological target being routinely called of virtual screening, or even, if this dependence is totally ruled out [32-33], the use of others CADD techniques is widely known in drug innovation [34-35], and properly in studies of phthalimide derivatives [36-37]. Despite being widely known but also over-highlighted here, the phthalimides belong to a very dynamic series of compounds with applications in many branches of the medicine [38], and as such, one of the potentials taken into account is the lipid-lowering effect [39]. By entering into the field of the CADD protocols [40], the use of the modeling approach without dependence of the biological target is a trustful path, and since it can be measured, it represents the proposition of the Quantitative Structure-Activity Relationship (QSAR) [41-42] on

the basis of statistic techniques. According to works of Ramos *et al*. [43-44], some successful QSAR models for phthalimide congeners were calibrated at the light of the AM1 Hamiltonian calculations supported by continuous solvent approaches.

Traditionally, since the initial works of Hansch and Fujita [45] up to the multidimensional approaches [46-48], the applicability of the QSAR formulations has been widely diffused among the medicinal community [49]. Even though with the QSAR embodied by higher dimensionality (5 or 6 levels) has provided excellent prediction models which aids effectively in the drug development [50], its superiority in comparison with the two-dimensional QSAR is not unanimous [51-52]. In some works, however, the prediction supported by 3DQSAR is slightly better than of the 2DQSAR model [53]. In addition to the parameters of the molecular orbital, the robustness of some QSAR models were tested and valued at light of electronic parameters derived from the quantum chemical calculations carried out in the routine of the Density Functional Theory (DFT) [54-55]. During the second half of the past century, although in view of the accurate elaboration of the first definitions of density functional by Hohenberg and Kohn [56], and soon later with the formalism divulged by Kohn

and Sham [57], the DFT has been severely criticized even though with a clear evolution with successful applications in many branches of science have been documented [58-59], of which we highlight the modeling of QSAR models at light of quantum mechanical descriptors [60-61]. The DFT formalism make possible to access a set of equations that describe the molecular electronic density [62-63]. By revisiting the foundation of the DFT, the exchange-correlation potential is defined as follows:

$$V_{xc}[\rho(r)] = \frac{\partial E_{xc}[\rho(r)]}{\partial \rho(r)} \quad (1)$$

The external potential, $V_{(r)}^{ext}$, namely the nucleus, the relationship between the variation of energy and the number of electrons (N) is given by:

$$\mu = \left(\frac{\delta E}{\delta N}\right)_{V_{(r)}^{ext}} \quad (2)$$

Once it has been self-named [64], the Fukui functions presented in the forms of the Equations (3) and (4) represent the neutral (N), cationic (N − 1, r) and anionic (N + 1, r) states, whereas the f^+ e f^- terms bring contents about a maximum possibility for molecular sites susceptible to be attacked by nucleophilic and electrophilic species, respectively.

$$f^+ \approx \rho(N + 1, r) - (N, r) \quad (3)$$

$$f^- \approx \rho(N, r) - (N - 1, r) \quad (4)$$

These equations can be rationalized to the DFT formalism as:

$$f(r) = \left(\frac{\partial \rho(r)}{\partial N}\right)_{V_{(r)}^{ext}} = \left(\frac{\partial \mu}{\partial v(r)}\right)_N \quad (5)$$

where μ represents the chemical potential. The Fukui functions display an observed response on the electronic density due to any infinitesimal perturbation in the total number of electrons (N) [64]. Indeed, the Equations (3) and (4) express the localization of local reactivity, but according to the Koopmans Theorem [65], reactivity can be theoretically measured by the Hartree-Fock ionization energy (I), i.e., the energy equivalent to the Highest Energy Molecular Bonding Orbital (HOMO):

$$I = -E_{HOMO} \quad (6)$$

Otherwise, the electronic affinity (A) is in line with the Lowest-Unoccupied Molecular Orbital (LUMO):

$$A = -E_{LUMO} \quad (7)$$

From these concepts, other molecular parameters can be determined, such as electronegativity (χ), hardness (η), softness (s), chemical potential (μ), and electropositivity index (ω) [66]:

$$\eta = \frac{-E_H + E_L}{2} \quad (8)$$

$$\sigma = \frac{1}{\eta} \quad (9)$$

$$\chi = \frac{-E_H - E_L}{2} \quad (10)$$

$$\mu = -\chi \quad (11)$$

$$\varpi = \frac{\mu^2}{2\eta} \quad (12)$$

The equations (10) and (11) are justified at the light of the DFT conception by the Equation (2):

$$\chi = -\mu = -\left(\frac{\delta E}{\delta N}\right) \quad (13)$$

Besides the Fukui indexes, f^+ e f^-, which have been used in QSAR studies [67-69], other very promising results have been yielded by using the following parameters: I, A, η, S, χ, μ and ω [70]. It is by means of this deployment of the DFT [71-72] that we can find new QSAR models by taking into account a set of phthalimide congeners widely studied, and of course, examining the possibility to compare with other reported works. Besides Ramos and Barros Neto [43-44], the QSAR investigations of phthalimides embodied a catalogue elaborated by Asif *et al*. [73] albeit in terms of using Fukui functions as QSAR descriptors still is innovative or few explored, this research insight has motivated us. Making some predicted remarks by the molecular modeling with dependence of the biological target, a study signed by Endo [74] concerning the treatment of the high levels of plasma of Low-Density Lipoprotein (LDL) yielded efficient outcomes [75]. Notwithstanding the endogenous synthesis of the cholesterol is ruled by the HMG-CoA reductase in a competitive process with allosteric effect or reversible phosphorylation, an increasing of adverse-effects caused by the use of statins is well-known, and therefore, the search for new alternative treatments for the high cholesterol levels with the inhibition of the HMG-CoA reductase enzyme is strongly recommended [76]. In spite of the molecular modeling with restrictions to the biological target is well-known [77], even so the application of the virtual screening tools may bring great understandings about the interactions formed by the amino acids of the HMG-CoA structure [78]. Accordingly, since our efforts converge to a docking investigation in association with the QSAR modeling, we hope to contribute with the molecular innovation of the phthalimide derivatives. Into the active site of the enzyme, despite the existence of polar interactions like hydrogen bonds as well as the nonpolar ones such as stacking and halogen bonds with σ-hole [79], the protocol to encompass them is based on the score of Gibbs free energy as presented by the Equation (14) [80]:

$$\Delta G_{(bind)} = \Delta G_{(vdW)} + \Delta G_{(HBond)} + \Delta G_{(Ele)} + \Delta G_{(def)} + \Delta G_{(solv)} \quad (14)$$

The contributions of the van der Waals (vdW), hydrogen bond (HBond), electrostatic (Ele), deformation (Def) and solvation energies (Solv) are taken into account. In synergism with the QSAR study, we are hoping that the docking simulations of the phthalimide derivatives into the HMG-CoA may provide a standard molecular modeling research work, although new horizons for drug innovation shall become more accessible.

2. Material and Methods

2.1 Computational procedure and details

Firstly, the structures of the phthalimides were built by using the GaussView program, and in a later stage all sorts of derivatives were submitted to an optimization process at the B3LYP/6-311++G(d,p) level of theory with all calculations carried out through the GAUSSIAN 03 program [81]. From these geometries, single-point calculations were performed to obtain the following descriptors: *i*) dipole moment (μ); the energies of the HOMO (E_H) and LUMO (E_L) orbitals; ChElPG and NBO atomic charges on the oxygen atom of the carbonyl

group (q-O(C=O)); electronegativity (χ); softness (σ) and absolute electrophilic index (ω) [82]. According to the set of Equations (6) up to (13), the DFT-based descriptors were determined. For the QSAR models, the Hierarchical Cluster Analysis (HCA), Principal Component Analysis (PCA) and Partial Least Squares (PLS) were developed through the Chemoface 1.61 program [83-84]. For HCA, PCA and PLS, the normalization of the numeric values of the descriptors were carried out. In PCA, the same matrix of the HCA procedure was used to obtain the scores and loadings graphs. For PLS, it was established the descriptors matrix **X** followed to the biological activity **Y** given in pT_{16} and pC_{16}. Lastly, the values of the values of the statistical parameters namely as RMSE, r^2_{cal}, r^2_{CV} and r^2_{test} were determined. The docking simulations were performed by means of the Autodock 4 (ADT4) [85] and Autodock Vina (Vina) [86] suite of programs. For the 2D and 3D visualizations of the ligand-biomacromolecule complexes, the PyMOL [87] and Discovery Studio Visualizer 4.0 [88]

softwares were used. From the Protein Data Bank (PDB), the crystallographic structure of the biological target used in the docking simulation was extracted with the code 2R4F. For the redocking, it was used the crystallographic ligand RIE, or 3R, 5R)-7-[2-(4-fluor-phenyl)-4-isopropyl-5-(4-methyl-benzylcarbamoyl)-2H-pyrazol-3-yl]-3, 5-dihidroxyheptanoic acid [89].

3. Results and Discussion

3.1 Unsupervised analyses and QSAR models

The geometries of all phthalimide compounds (**1**-**18**) optimized with B3LYP/6-311++G(d,p) calculations are exhibited in the Figure 2, whose values of the quantum chemical descriptors are listed in Table 2.
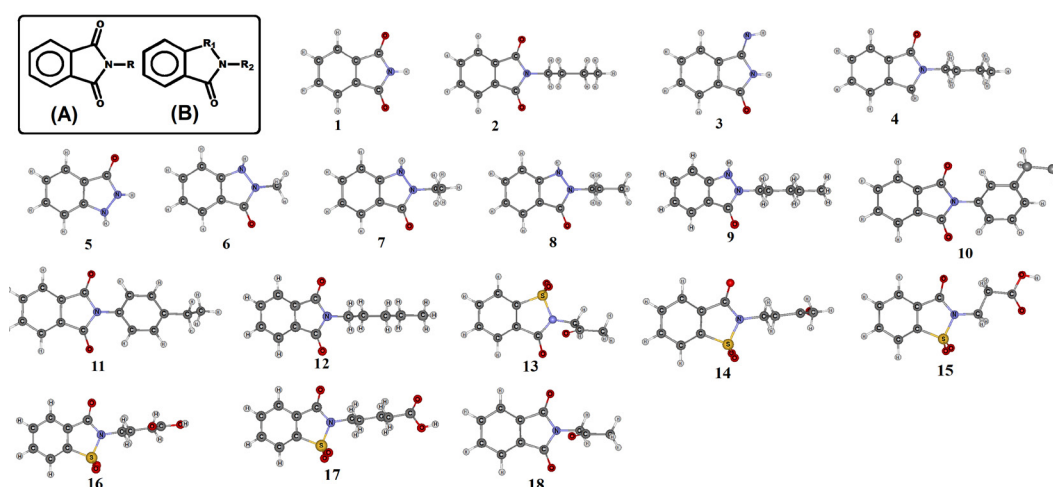
Fig. 2. Optimized geometries of the phthalimides obtained from the B3LYP/6-311++G(d,p) calculations.

Because the standard statistics-based biological activities data preprocessing was the first step to be fulfilled, the dendrogram for the values of C_{16} and T_{16} are presented in Figure 3. By the identification of Euclidean distance in the threshold between 18 and 30 wherein two (**G4** and **G5**) and three (**G1**, **G2** and **G3**) clusters are recognized. For the HCA study of the C_{16} data, the **G1** cluster consist of a single representation embodied by the **6** and **9** compounds as well

as the **16** and **18** ones, by which the C_{16} values framed in 70% are obtained and once these are the remaining biological activities, thus they are one of the median active congeners. It is worthy to highlight the missing of structural relationships derived from either the pharmacophore contributions, or substituents groups, particularly aiming to provide a better similarity projection.
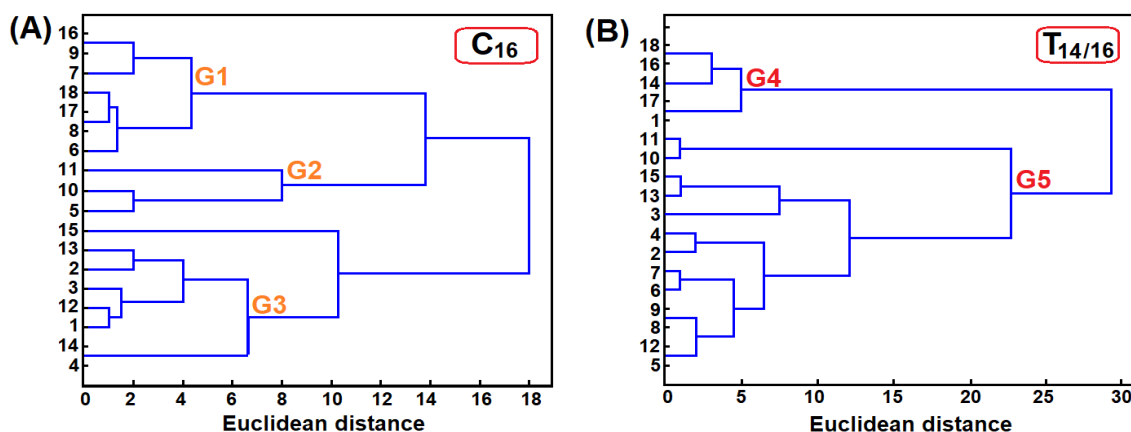
Fig. 3. HCA clusters for the set of phthalimide derivatives with hypolipidemic activity expressed as follows: **A** = C_{16} and **B** = $T_{14/16}$ from the value gathered in Table 1.

Regarding the **G2** cluster, in which the **5**, **10** and **11** congeners are grouped, they are the less active derivatives because their values of biological activity are ranged by 82-89 %. Regardless the **5** compound, the **10** and **11** congeners bring the same R_1 substituent group (C=O) albeit the difference is just in the C_2H_5 group linked (*m* or *p*) to the aromatic ring.

Among them, however, there is no evident structural similarity concerning the **5** compound. In turn, **G3** encompasses the compounds with high biological activity, and in fact, it was not possible to identify any molecular similarity because this cluster is the biggest one.

Table 2. Values of the descriptors derived from B3LYP/6-311++G(d,p) calculations.

	μ	E_H	E_L	q-O(C=O)[1]	q-O(C=O)[2]	χ	σ	ω
1	3.1121	-0.28586	-0.09921	-0.549	-0.513	0.1925	10.7152	51.8894
2	2.0884	-0.27559	-0.09364	-0.561	-0.484	0.1846	10.9920	23.9704
3	1.4722	-0.27518	-0.08551	-0.566	-0.534	0.1803	10.5446	11.4273
4	4.1411	-0.24805	-0.04609	-0.627	-0.559	0.1470	9.9029	84.9787
5	4.4090	-0.23578	-0.05785	-0.604	-0.612	0.1468	11.2403	109.2525
6	4.2922	-0.22807	-0.05151	-0.626	-0.580	0.1398	11.3276	104.3790
7	4.2680	-0.22632	-0.05020	-0.629	-0.579	0.1382	11.3558	103.4400
8	4.2479	-0.22536	-0.04951	-0.630	-0.583	0.1374	11.3733	102.6027
9	4.2145	-0.22499	-0.04932	-0.630	-0.584	0.1371	11.3845	101.1503
10	2.1610	-0.24673	-0.09524	-0.547	-0.518	0.1709	13.2000	30.8445
11	1.8977	-0.24280	-0.09514	-0.546	-0.522	0.1689	13.5446	24.2984
12	2.1143	-0.27530	-0.09363	-0.561	-0.488	0.1844	11.0089	24.6156
13	1.8904	-0.26919	-0.08755	-0.569	-0.490	0.1784	11.0107	19.6740
14	5.7555	-0.26533	-0.09130	-0.577	-0.504	0.1783	11.4923	190.3781
15	4.7871	-0.29088	-0.09273	-0.575	-0.275	0.1918	10.0933	115.6804
16	3.0256	-0.28807	-0.08981	-0.575	-0.503	0.0593	10.0877	46.1866
17	4.3585	-0.28521	-0.09081	-0.575	-0.480	0.0596	10.2880	101.9125
18	1.8367	-0.26708	-0.09447	-0.559	-0.498	0.1807	11.5868	19.5446

Values of μ are given in Debye (D); Values of E_H, E_L, χ, σ and ω are given in Hartree; q-O(C=O)[1] and q-O(C=O)[2] atomic charges obtained from NBO and ChElPG calculations, respectively, and whose values are given in Electronic Units (e.u.).

With respect to the dendrogram of the T_{16} activities, Figure 3-(**B**), even by fixing the Euclidean distance of 23.0, two groups were clearly identified, namely **G4** and **G5**. In the first, **G4**, the compounds with the lowest activity values are hosted, in other words, the more active ones. Overall, most of these congeners carry as main feature the presence of two substituent groups, amazingly one polar and other nonpolar. From the Euclidean distance fixed at 5.0, the Figure 3-(**B**) exhibits the main similarity among all compounds regarding the high E_L values as well as by taking into account the NBO and ChElPG atomic charges, low values were computed in qC=O. The Figure 4-(**A**) shows the HCA analysis for the descriptors listed in Table 2, and it can be seen, no direct relationship with the biological activities can be firmed.

If we consider both PC1 and PC2 pictured in the Figure 4-(**B**) [90], where the first vector accounts 95.97% whereas the

second one holds the 4.03% of the residual variance, amazingly the total variance could be encompassed. Regardless if pC_{16} and pT_{16} are taken into account, all compounds are located in the negative site of PC1, although in the high biological activity accounted by the pC_{16} data, the compound labeled by **3** is localized in the positive extreme of PC2 axis. Note that, the overlaying of the loading and scores into the biplot graph, Figure 4-(**B**) [90], only the softness (σ) and absolute electrophilic index (ω) match with the reducing of the T_{16} levels, such as when the **16** and **1** compounds are highlighted, for instance. There would be no similarity between these compounds actually, in which the R1 and R2 substituent groups are quite different, even so the values of their polarities are practically the same.
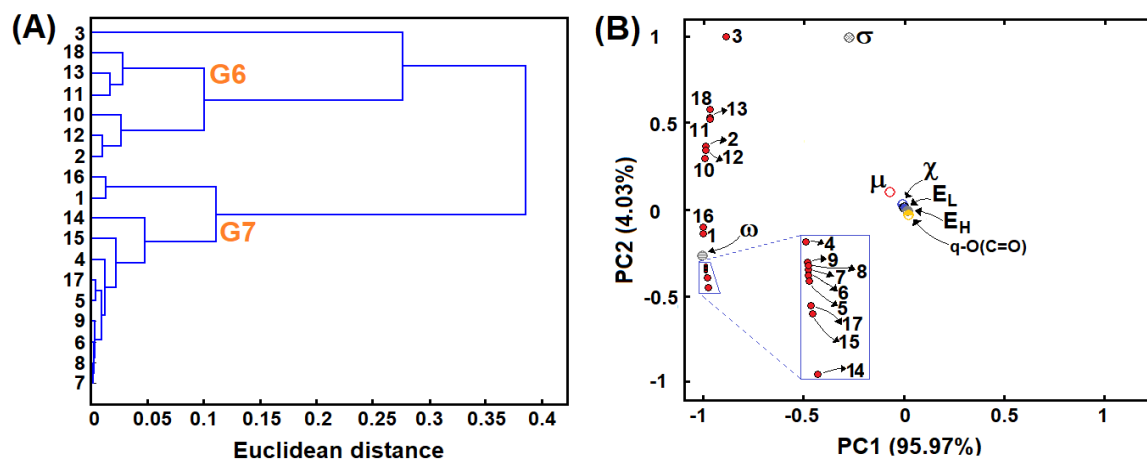
Fig. 4. **(A)**: HCA clusters for the set of descriptors (Table 2) of the phthalimide derivatives; **(B)**: PCA graphs with a biplot projection (scores and loadings) derived from the set of descriptors (Table 2).

In the past, the results signed by Ramos and Barros Neto [43] have served as references to the current ones debated here, although it should be highlighted that they used a smaller number of molecules, and accordingly the values of C_{16} and T_{16} are less varied on the average by which a better statistical model might be yielded [91]. For generating the QSAR models based on PLS algorithm, the data listed in Table 1 and the results of the descriptors gathered in Table 2 were used. The normalization procedure was assessed in the **X** independent variable whereas the dependent one, that is **Y**, this is responsible by the biological activity [92]. Moreover, 16% of the samples were conditioned as belonging to the test set for the leave-one-out routine procedure [93-94]. After the calibration process, the results are graphically illustrated in the Figure 5-(**A**), in which the r^2_{cal} calibration coefficient value of 0.937 followed by the RMSE result of 0.017 can be considered very satisfactory (Table 3). In view of this, our results are in full agreement and even more trustful in comparison to those reported by Ramos and Barros Neto [43]. Of course these results were achieved by taking into account

the charge density on oxygen of the carbonyl group at light of the ChEIPG calculation, although if the NBO results are included into the model, the calibration is slightly less expressive whereas the validation is extremely poor (Table 3). For the PLS analysis carried out for the pT_{16} data, see Figure 5-(**B**), the QSAR model is less efficient, such as is graphically illustrated as well as according to the RMSE, r^2_{cal}, r^2_{CV} and r^2_{test} results organized in Table 3.

Table 3. Values of the chemometric parameters [95].

PLS		Parameters			
		pT_{16}		pC_{16}	
		ChEIPG	NBO	ChEIPG	NBO
Calibration	RMSE	0.035	0.057	0.017	0.022
	r^2_{cal}	0.881	0.687	0.937	0.891
CV	RMSE	0.095	0.286	0.048	0.071
	r^2_{CV}	0.287	0.068	0.591	0.487
Validation	RMSE	0.603	0.897	0.036	0.127
	r^2_{test}	0.186	0.563	0.850	0.000
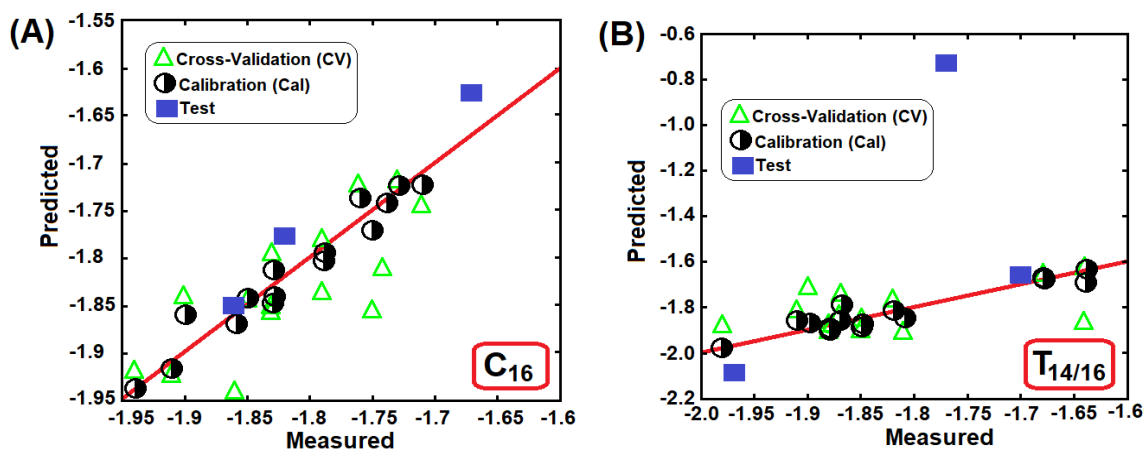
Fig. 5. (**A**): PLS model for the C_{16} data; (**B**): PLS model for the $T_{14/16}$ data.

As is well known [96], the standard data for the correlation coefficient of multiple determination in QSAR studies is a threshold of 0.6, and as such, our result of 0.850 for C_{16} is quite efficient. The Equations (15) and (16), which represent

the predicted and measured values of C_{16} and $T_{14/16}$ were generated through the linear analyses of the Figure 6.(**A**) and (**B**).
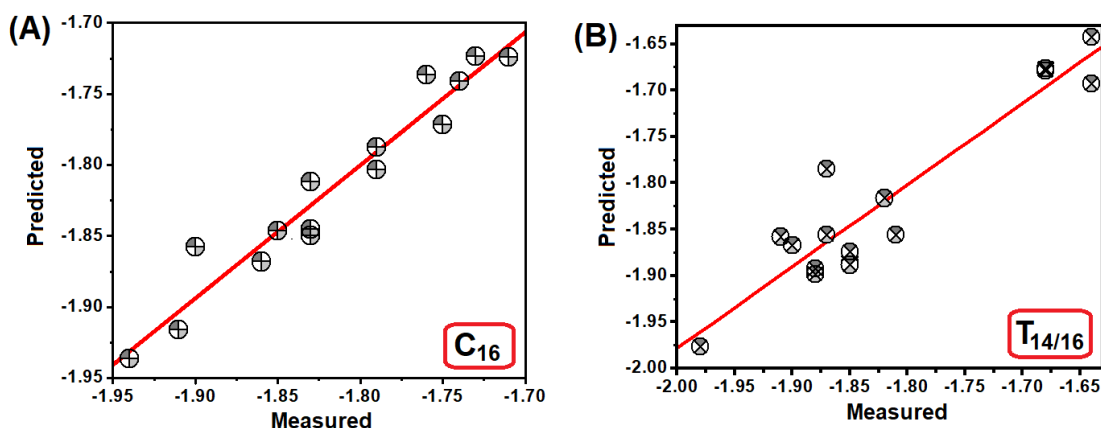
Fig. 6. (**A**): Predicted and measured values of C_{16}; (**B**): Predicted and measured values of $T_{14/16}$.

$$C_{16(predicted)} = 0.937\ C_{16(measured)} - 0.114 , r^2 = 0.97 \quad (15)$$

$$T_{14/16(predicted)} = 0.881\ T_{14/16(measured)} - 0.215 , r^2 = 0.94 \quad (16)$$

The use of atomic charges [97] in molecular modeling investigations is widely established [98], although here, our

results showed that one specific approach can provide a more efficient QSAR model, and therefore, the most robust linear relationship was reached through the values of the ChElPG scheme.

3.2 Virtual screening studies

The display of the docking procedure for the RIE ligand are presented in Figure 7. Through the RMSD result of 0.221, the RIE compound binds precisely in the coordinate of the active site of the HMG-CoA reductase. Moreover, in line with the Vina-score result of -9.1 Kcal.mol^{-1}, it is also reliable to state that a biosupermolecule structure may be fairly formed, by which, the accuracy of the docking protocol is certified.
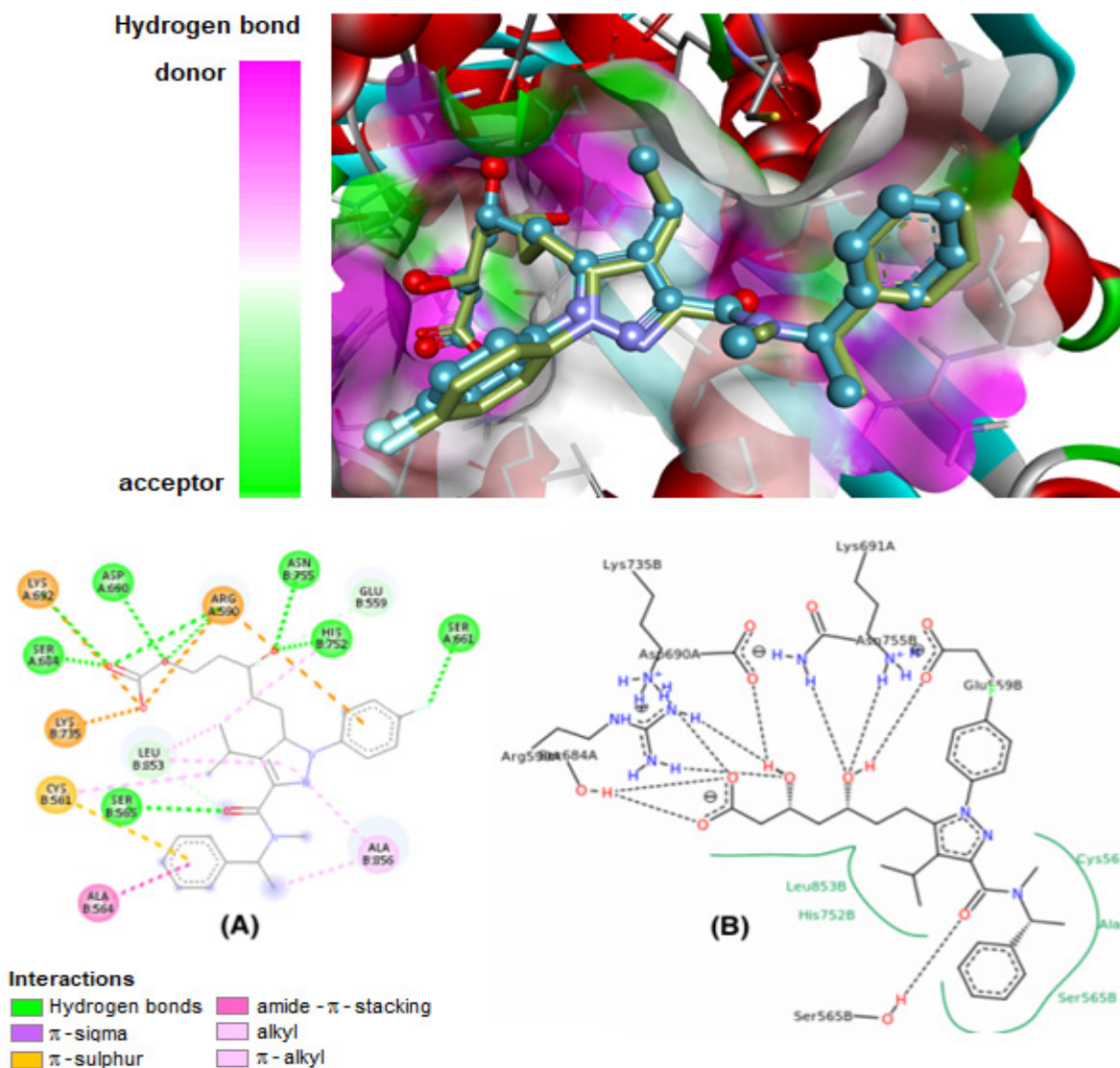
Fig. 7. Ligands redocked in the active site of the HMG-CoA enzyme (original ligand in blue as well as the redocking result in green). (**A**) and (**B**) are illustrations of the redocking and original ligand pose.

Framed in a 2D view, the intermolecular interactions can be visualized, wherein the results depicted in Figure 7(**A**) and Figure 7(**B**) are quite similar. These results are conditioned to the redocking result and the original ligand configuration, and as such, it is worthy be noted the C=O⋯H−O and C−O⋯H−N hydrogen bonds formed between the carbonyl and serine amino acid (SER-B-565) or even between the ester and amidic hydrogen of lysine (LYS-B-735), respectively. Among the 36 interactions clearly identified, 14 of them are hydrogen bonds, the other 14 ones present a purely electrostatic profile, and the other 8 types are nonpolar or hydrophobic. In Table 4 are organized the docking score results related to the 18 phthalimide congeners on the HGM-CoA reductase. As is widely known, the more fitted conformation provides the lowest binding energy, and therefore, the compounds labeled by **10**, **15**, **16** and **17** are those ones with more stable score

energy results. In according with this statement, the Figure 8 and Figure 9 exhibit the hydrogen bonds formed on these congeners when they bind with the HGM-CoA reductase.

Table 4. Score values for the docking simulations.

N	Vina Score (ΔG)*	N	Vina Score (ΔG)*	N	Vina Score (ΔG)*
1	-6.5	**7**	-5.4	**13**	-6.2
2	-5.8	**8**	-5.4	**14**	-6.5
3	-6.5	**9**	-5.8	**15**	-6.8
4	-5.6	**10**	-6.9	**16**	-7.0
5	-6.4	**11**	-6.4	**17**	-7.0
6	-5.6	**12**	-6.0	**18**	-5.9

*All values in Kcal.mol^{-1}.
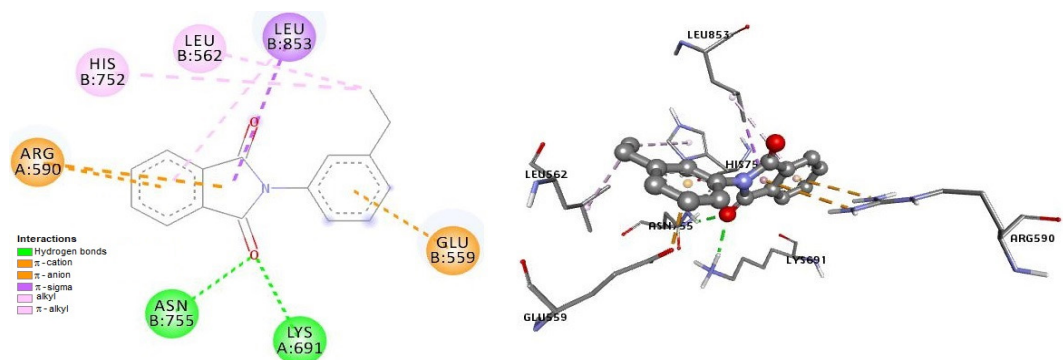
(10)
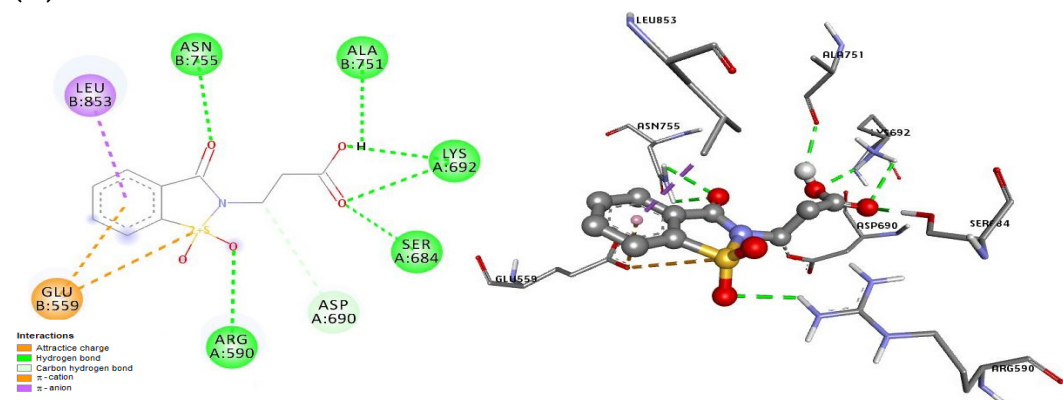
(15)

Fig. 8. Identification of the interaction sites for the ligand-enzyme complex formed by the (**10**) and (**15**) congeners.
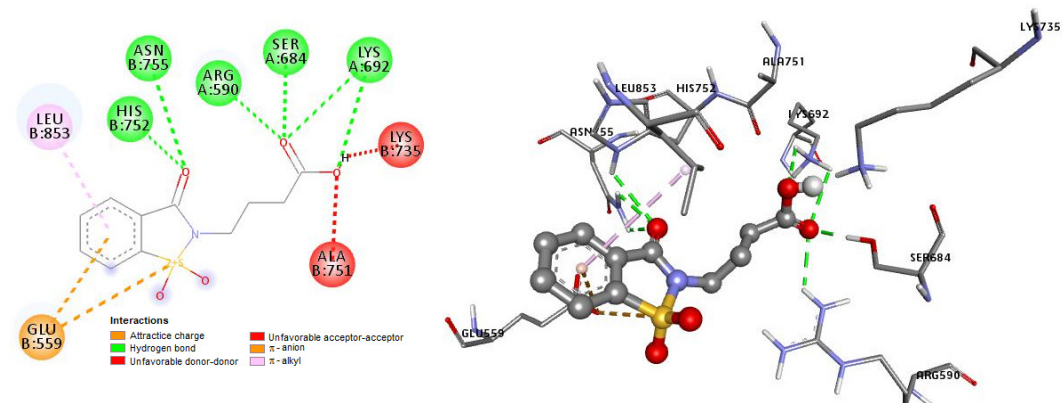
(16)
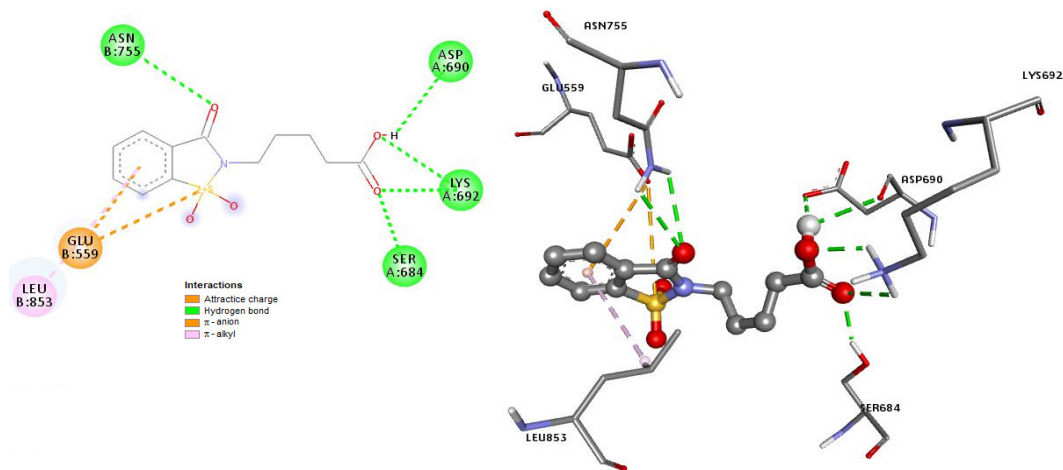
(17)

Fig. 9. Identification of the interaction sites for the ligand-enzyme complex formed by the (**16**) and (**17**) congeners.

In order to evidence the robustness of the docking score, the Figure 10 (**A**) and Figure 10 (**B**) exhibit the relationship between a selected group of phathalimides, precisely those ones whose ΔG results are in good agreement with the biological activities, i.e. pC_{16} and $pT_{14/16}$.
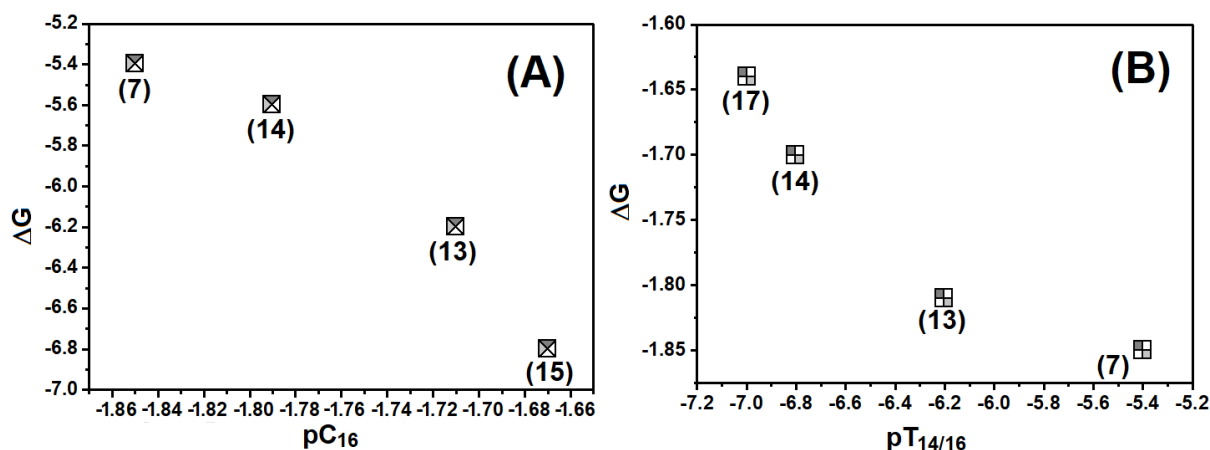
Fig. 10. Relationships between the docking score and the biological activities.

Note that a fairly linear trend is established, and in an overview, the most stable docking score corroborate with the most efficient reductions of C_{16} and $T_{14/16}$ effectively, by which leads us to affirm that the **17** congener provides the best conformation at all. Of course the great aim is not to declare that all compounds sustain this relationship, but it is worthy that since these representative profiles occur, the docking algorithm is well valued in this regard. Among all congeners carefully analyzed, **15** is that one with a bright pharmacological prominence due to the %C_{16} datum of 47,

although the docking score found was -6.8, which is the not the most stable in comparison with all other results herein presented.

Regarding to **16** and **17**, even though their score results of -7.0 are equals, the most interactions with the same amino acid residues have distinct interaction distances. Even by taking into account these differences, it can be seen that repulsive interactions can be observed in **16**, and actually these are unfavorable (painted in red) for the docking.

Table 5. Interaction between the **15** ligand on the HMG-CoA reductase enzyme.

N	Type	R (distance)	Residues	Type	R (distance)	Residues
1	Hydrogen bond[a]	2.78	A:ARG590	Hydrogen bond	2.26	B:ALA751
2	Hydrogen bond[a]	1.95	A:SER684	Hydrogen bond	3.42	A:ASP690
3	Hydrogen bond[a]	2.65	A:LYS692	Electrostatic	5.39	B:GLU559
4	Hydrogen bond[a]	2.28	A:LYS692	Electrostatic	4.31	B:GLU559
5	Hydrogen bond[a]	2.82	B:ASN755	Hydrophobic	3.73	B:LEU853
6	Hydrogen bond[a]	2.60	B:ASN755	—	—	—

Distance values (R) in Å.; [a] Hydrogen bond model: Ref. [99-102]

As it is vastly known as Sortis, Torvast or Atorlip, the atorvastatin as inhibitor is one of the greatest blockbusters of the bigpharma. Well, Stanley *et al.* [103] have demonstrated the biological potentiality of the drug based on the docking simulations by taking into account a serial of congeners with several statins. By analyzing the pharmacophore contributions at the light of docking, Tripathi *et al.* [104] have discussed a satisfactory relationship between bioreceptor-atorvastatin framed by the fluorine atom, wherein the search for an optimized compound based on others pharmacophore

contributions has become counterproductive. In this context, the current study aims also to revisit the docking results for atorvastatin in the active site of the HMG-CoA reductase enzyme.

By carrying out the regime of the Vina protocol, the score result of -9.9 Kcal.mol^{-1} was computed. The Figures 11 (**A**) and (**B**) as well as the Table 6 expose the values of the hydrogen bond distances achieved in the bioreceptor (HMG-CoA reductase)⋯ligand(atorvastatin) complex.

Table 6. Main interactions on the HMG-CoA⋯atorvastatin complex

N	Type	R (distance)	Residues	Type	R(distance)	Residues
1	Hydrogen bond	3.01	O23⋯A:ASP690	Hydrogen bond	2.66	A:LYS692⋯O22
2	Hydrogen bond	2.97	A:ARG590⋯F13	Hydrogen bond	2.88	A:LYS692⋯O22
3	Hydrogen bond	2.14	A:ARG590⋯O23	Hydrogen bond	2.39	B:SER565⋯O36
4	Hydrogen bond	2.35	A:ARG590⋯O23	Hydrogen bond	2.11	B:LYS735⋯O21
5	Hydrogen bond	2.55	A:ARG590⋯O22	Hydrogen bond	2.52	B:HIS752⋯O41
6	Hydrogen bond	2.75	A:SER661⋯F13	Hydrogen bond	2.30	B:ASN755⋯O41
7	Hydrogen bond	1.91	A:SER684⋯O22	—	—	—

Distance values (R) in Å.

Fig. 11. Docking of the atorvastatin in the active site of the HMG-CoA reductase (**A**) and the 2D representation of the hydrogen bond interactions (**B**).

It is, truly, a large set of hydrogen bonds formed between the atorvastatin and the HMG-CoA reductase enzyme. Even though the immediate interaction between the fluorine atom may be a decisive factor related to the binding with both arginine and serine amino acids, if the distance is taken into account, in particular the result of 1.91 Å for O···H, the fluorine not behaves as a reliable center to form stronger hydrogen bonds. In this same amino acid, however, the fluorine forms a hydrogen bond with a long distance, whose result is 2.75 Å. Furthermore, in arginine, the oxygen stands as the main proton acceptor center to form hydrogen bond interactions, wherein the distance value of 2.14 Å is very shorter than 2.97 Å furnished by the fluorine.

4. Conclusions

This theoretical work was carried out in order to propose QSAR models and virtual screening tests involving docking simulations on the HMG-CoA enzyme for phthalimide congeners with hypolipidemic activity. The set of descriptors derived from the DFT formalism have yielded satisfactory statistical profiles, mainly by considering the absolute electrophilic index, softness and ChElPG atomic charges. Regarding to the docking simulations, besides the validation of the redocking procedure has been successfully performed, the Vina version of the AutoDock sets of protocols behaves more efficient with a broader projections of poses around the pocket active site of the HMG-CoA. In this context, not merely regarding the perspective of the proton accepting center to form hydrogen bonds but focusing into the active site of the amino acids, the serine and arginine are the benchmarks in this regard. Among the whole set of congeners, the structures labeled as **16** and **17** furnished the best score results, although those ones related to **15** were considered due to the fact of the shorter interaction distances have been computed, whose profile agrees to that already known for the atorvastatin. In view of this, the docking results revealed new insights to form interaction with the arginine and serine amino acids.

Supporting Information

Scores and loadings of the PCA. Additional information of the chemometric procedure. Coordinates of the optimized geometries of the phthalimide congeners obtained through the B3LYP/6-311++G(d,p) calculations used in the QSAR studies.

References and Notes

[1] https://www.who.int/health-topics/cardiovascular-diseases/#tab=tab_1, access March 2021.

[2] Reamy, B. V.; Williams, P. M.; Kuckel, D. P. *Prim. Care* **2018**, *45*, 25. [Crossref]

[3] Rique, A. B. R.; Soares, E. A.; Meirelles, C. M. *Rev. Bras. Med. Esp.* **2002**, *8*, 244. [Crossref]

[4] Institute of Medicine. A population-based policy and systems change approach to prevent and control hypertension. Washington, DC: The National Academies Press, 2010. [Crossref]

[5] Khanji, M. Y.; Bicalho, V. V.; van Waardhuizen, C. N.; Ferket, B. S.; Petersen, S. E.; Hunink, M. G. *Ann. Intern. Med.* **2016**, *10*, 713. [Crossref]

[6] Dake, A. W.; Sora, N. D. *Am. J. Med. Sci.* **2016**, *351*, 361. [Crossref]

[7] Ikonen, E. *Curr. Opin. Cell. Bio.* **2018**, *53*, 77. [Crossref]

[8] Batista, R. M.; Zandonade, E.; Roelke, L. H.; Emmerich, A. O.; Rosetti, E. P.; Molina, M. C. B.; Santos Neto, E. T. *J. Vasc. Bras.* **2011**, *10*, 229. [Crossref]

[9] Abramson, J.; Rosenberg, H. G.; Jewell, N.; Wright, J. M. *Lancet* **2017**, *389*, 1097. [Crossref]

[10] PInal-Fernandez, I. P.; Casal-Dominguez, M.; Mammen, A. L. *Med. Clín.* **2018**, *150*, 398. [Crossref]

[11] Brown, A. G.; Smale, T. C.; King, T. J.; Hasenkamp, R.; Thompson, R. H. *J. Chem. Soc. Perkin.* **1976**, *1*, 1165. [Crossref]

[12] Campo, V. L.; Carvalho, I. *Quim. Nova* **2007**, *30*, 425. [Crossref]

[13] Curran, M. P.; Goa, K. L. *Drugs* **2003**, *63*, 685. [Crossref]

[14] Sharma, U.; Kumar, P.; Kumar, N.; Singh, B. *Mini Rev. Med. Chem.* **2010**, *10*, 678. [Crossref]

[15] Sena, V. L. M.; Srivastava, R. M.; Silva, R. O.; Lima, V. L. M. *Il Farmaco* **2003**, *58*, 1283.

[16] Pin, B. L.; Tavares, L. A. *Braz. J. Prod. Eng.* **2016**, *2*, 11.

[17] Chapman Jr., J. M.; Cocolas, G. H.; Hall, I. H. *J. Med. Chem*. **1979**, *22*, 1399. **[Crossref]**

[18] Hall, I. H.; Chapman, J. M.; Cocolas, G. H. *J. Pharm. Sci*. **1981**, *70*, 326. **[Crossref]**

[19] Chapman Jr., J. M.; Wyrick, S. D.; Voorstad, P. J.; Maguire, J. H.; Cocolas, G. H.; Hall, I. H. *J. Pharm. Sci*. **1984**, 73, 1482. **[Crossref]**

[20] Chapman Jr., J. M.; Cocolas, G. H.; Hall, I. H. *J. Med. Chem*. **1983**, *26*, 243. **[Crossref]**

[21] Murthy, A. R.; Wong, O. T.; Reynolds, D. J.; Hall, I. H. *Pharm. Res*. **1987**, *4*, 21. **[Crossref]**

[22] Wyrick, S. D.; Voorstad, P. J.; Cocolas, G. H.; Hall, I. H. *J. Med. Chem*. **1984**, *27*, 768. **[Crossref]**

[23] Chapman Jr., J. M.; Voorstad, P. J.; Cocolas, G. H.; Hall, I. H. *J. Med. Chem*. **1983**, *26*, 237. **[Crossref]**

[24] Tralau-Stewart, C. J.; Wyatt, C. A.; Kleyn, D. E.; Ayad, A. *Drug Discov. Today* **2009**, *14*, 95. **[Crossref]**

[25] Frearson, J.; Wyatt, P. *Expert. Opin. Drug Discov*. **2010**, *5*, 909. **[Crossref]**

[26] Morgan, S.; Grootendorst, P.; Lexchinef, J.; Cunningham, C.; Greyson, *D. Health Pol*. **2011**, *100*, 4. **[Crossref]**

[27] Van Norman, G. A. *JACC: Basic Trans. Sci*. **2016**, *1*, 170. **[Crossref]**

[28] DiMasi, J. A.; Hansen; R. W.; Grabowski, H. G. *J. Health Econ*. **2003**, *22*, 151. **[Crossref]**

[29] DiMasi, J. A. *PharmacoEconomics* **2002**, *20*, 1. **[Crossref]**

[30] Ou-Yang, S. -S.; Lu, J. -Y.; Kong, X. -Q.; Liang, Z. -J.; Luo, C.; Jiang, H. *Acta Pharm. Sin*. **2012**, *33*, 1131. **[Crossref]**

[31] Baig, M. H.; Ahmad, K.; Roy, S.; Ashraf, J. M.; Adil, M.; Siddiqui, M. H.; Khan, S.; Kamal, M. A.; Provazník, I.; Choi, I. *Curr. Pharm. Des*. **2016**, *22*, 572. **[Crossref]**

[32] Viana, J. O.; Félix, M. B.; Maia, M. S.; Serafim, V. L.; Scotti, L.; Scotti, M. T. *Braz. J. Pharm. Sci*. **2018**, *54*, 1. **[Crossref]**

[33] Neves, B. J.; Braga, R. C.; Melo-Filho, C. C.; Moreira-Filho, J. T.; Muratov, E. N.; Andrade, C. H. *Front. Pharmacol*. **2018**, *9*, 1275. **[Crossref]**

[34] Kore, P. P.; Mutha, M. M.; Antre, R. V.; Oswal, R. J.; Kshirsagar, S. S. *Open. J. Med. Chem*. **2012**, *2*, 139. **[Crossref]**

[35] Macalino, S. J. Y.; Gosu, V.; Hong, S.; Choi, S. *Arch. Pharm. Res*. **2015**, *38*, 1686. **[Crossref]**

[36] Othman, I. M. M.; Gad-Elkareem, M. A. M.; El-Naggar, M.; Nossier, E. S.; Amr, A. E. -G. E.; J. *Enzyme Inhib. Med. Chem*. **2019**, *34*, 1259. **[Crossref]**

[37] Ungwitayatorn, J.; Matayatsuk, C.; Sothipatcharasai, P. *ScienceAsia* **2001**, *27*, 245. **[Crossref]**

[38] da Silva Jr., J. G.; Holanda, V. N.; Gambôa, D. S. R.; do Monte, T. V. S.; de Araújo, H. D. A.; do Nascimento Jr., J. A. A.; Araújo, V. F. S.; Callôu, M. A. M.; Assis, S. P. O.; Lima, V. L. M. *Am. J. Biomed. Sci. Res*. **2019**, *3*, 378. **[Crossref]**

[39] Hall, I. H.; Wong, O. T.; Wyrick, S. D. *Pharm. Res*. **1988**, *5*, 413. **[Crossref]**

[40] Bisht, N.; Singh, B. K. *Int. J. Pharm. Sci. Res*. **2018**, *9*, 1405. **[Crossref]**

[41] Muhammad, U.; Uzairu, A.; Arthur, D. E. *J. Anal. Pharm. Res*. **2018**, *7*, 240. **[Crossref]**

[42] Cherkasov, A.; Muratov, E. N.; Fourches, D.; Varnek, A.; Baskin, I. I.; Cronin, M.; Dearden, J.; Gramatica, P.; Martin, Y. C.; Todeschini, R.; Consonni, V.; Kuz'min, V. E.; Cramer, R.; Benigni, R.; Yang, C.; Rathman, J.; Terfloth, L.; Gasteiger, J.; Richard, A.; Tropsha, A. *J. Med. Chem*. **2014**, *57*, 4977. **[Crossref]**

[43] Ramos, M. N.; Neto, B. B. *J. Comput. Chem*. **1990**, *11*, 569. **[Crossref]**

[44] da Silva, A. G.; Ramos, M. N. *J. Braz. Chem. Soc*. **2012**, *23*, 1747. **[Crossref]**

[45] Hansch, C.; Fujita, T. *J. Am. Chem. Soc*. **1964**, *86*, 1616. **[Crossref]**

[46] Vedani, A.; Dobler, M. *Quant. Struct. -Act. Relat*. **2002**, *21*, 382. **[Crossref]**

[47] Lill, M. A. *Drug Discov. Today* **2007**, *12*, 1013. **[Crossref]**

[48] Wang, T.; Yuan, X. -S.; Wu, M. -B.; Lin, J. -P.; Yang, L. -R. *Expert Opin. Drug Discov*. **2017**, *12*, 769. **[Crossref]**

[49] Alves, V. M.; Braga, R. C.; Muratov, E. N.; Andrade, C. H. *Quim. Nova* **2018**, *41*, 202. **[Crossref]**

[50] Damale, M. G.; Harke, S. N.; Khan, F. A. K.; Shinde, D. B.; Sangshetti, J. N. *Mini Rev. Med. Chem*. **2014**, *14*, 35. **[Crossref]**

[51] Ghanbarzadeh, S.; Ghasemi, S.; Shayanfar, A.; Ebrahimi-Najafabadi, H. *EXCLI J*. **2015**, *14*, 484. **[Crossef]**

[52] Shayanfar, A.; Ghasemi, S.; Soltani, S.; Asadpour-Zeynali, K.; Doerksen, R. J.; Jouyban, A. *Med. Chem*. **2013**, *9*, 434. **[Crossref]**

[53] Veras, L. S.; Arakawa, M.; Funatsu, K.; Takahata, Y. *J. Braz. Chem. Soc*. **2010**, *21*, 872. **[Crossref]**

[54] Kryachko, E. S.; Ludeña, E. V. *Phys. Rep*. **2014**, *544*, 123. **[Crossref]**

[55] Mardirossian, N.; Head-Gordon, M. *Mol. Phys*. **2017**, *115*, 2315. **[Crossref]**

[56] Hohenberg, P.; Kohn, W. *Phys. Rev*. **1964**, *136*, B864. **[Crossref]**

[57] Kohn, W.; Sham, L. J. *Phys. Rev*. **1965**, *140*, A1133. **[Crossref]**

[58] van Mourik, T.; Bühl, M.; Gaigeot, M. -P. *Philos. Trans. A Math. Phys. Eng. Sci*. **2014**, *372*, 20120488. **[Crossref]**

[59] Herrera, M.; Serra, R. M.; D'Amico, I. *Sci. Rep*. **2017**, *7*, 4655. **[Crossref]**

[60] Tozer, D. J.; De Proft, F. *J. Chem. Phys*. **2007**, *127*, 034108. **[Crossref]**

[61] Hussain, I.; Bania, K. K.; Gour, N. K.; Deka, R. C. *Chem. Selec*. **2016**, *1*, 4973. **[Crossref]**

[62] Ayers, P. W.; Melin, J. *Theor. Chem. Acc*. **2007**, *117*, 371. **[Crossref]**

[63] van Damme, S.; Bultinck, P. *J. Comput. Chem*. **2009**, *30*, 1749. **[Crossref]**

[64] Fukui, K. *Science* **1982**, *218*, 747. **[Crossref]**

[65] Koopmans, T. *Physica* **1934**, *1*, 104. **[Crossref]**

[66] Wazzan, N. A.; Mahgou, F. M. *Open J. Phys. Chem*. **2014**, *4*, 6. **[Crossref]**

[67] Djeradi, H.; Rahmouni, A.; Cheriti, A. *J. Mol. Model*. **2014**, *20*, 2476. **[Crossref]**

[68] Rahmouni, A.; Touhami, M.; Benaissa, T. *Int. J. Chemominfor. Chem. Eng*. **2017**, *6*, 31. **[Crossref]**

[69] Hazhazi, H.; Melkemi, N.; Salah, T.; Bouachrine, M. *Heliyon* **2019**, *5*, e02451. **[Crossref]**

[70] Sayiner, H. S.; Abdalrahm, A. A. S.; Basaran, M. A.; Kovalishyn, V.; Kandemirli, F. *Med. Chem.* **2018**, *14*, 253. **[Crossref]**

[71] Parr, R. G.; Yang, W. *J. Am. Chem. Soc.* **1984**, *106*, 4049. **[Crossref]**

[72] Ayers, P. W.; Levy, M. *Theor. Chem. Acc.* **2000**, *103*, 353. **[Crossref]**

[73] Imran, M.; Bisht, A. S.; Asif, M. *Acta Sci. Pharm. Sci.* **2019**, *3*, 51.

[74] Endo, A. *Proc. Jpn. Acad. Ser. B Phys. Biol. Sci.* **2010**, *86*, 486. **[Crossref]**

[75] Wadhera, R. K.; Steen, D. L.; Khan, I.; Giugliano, R. P.; Foody, J. M. *J. Clin. Lipidol.* **2016**, *10*, 472. **[Crossref]**

[76] Luo, J.; Yang, H.; Song, B.-L. *Nat. Rev. Mol. Cell Bio.* **2020**, *21*, 225. **[Crossref]**

[77] Ghasemi, G.; Nirouei, M.; Shariati, S.; Abdolmaleki, P.; Rastgoo, Z. *Arab. J. Chem.* **2016**, *9*, S185. **[Crossref]**

[78] Marahatha, R.; Basnet, S.; Bhattarai, B. R.; Budhathoki, P.; Aryal, B.; Adhikari, B.; Lamichhane, G.; Poudel, D. K.; Parajuli, N. bioRxiv, **2020**, 1. **[Crossref]**

[79] Bissantz, C.; Kuhn, B.; Stahl, M. *J. Med. Chem.* **2010**, *53*, 5061. **[Crossref]**

[80] Hill, A. D.; Reilly, P.J.; *J. Comput. Chem.* **2008**, *29*, 1131. **[Crossref]**

[81] Gaussian 03, Revision C.01, Frisch, M. J.; Trucks, G. W.; Schlegel, H. B.; Scuseria, G. E.; Robb, M. A.; Cheeseman, J. R.; Montgomery Jr., J. A.; Vreven, T.; Kudin, K. N.; Burant, J. C.; Millam, J. M.; Iyengar, S. S.; Tomasi, J.; Barone, V.; Mennucci, B.; Cossi, M.; Scalmani, G.; Rega, N.; Petersson, G. A.; Nakatsuji, H.; Hada, M.; Ehara, M.; Toyota, K.; Fukuda, R.; Hasegawa, J.; Ishida, M.; Nakajima, T.; Honda, Y.; Kitao, O.; Nakai, H.; Klene, M.; Li, X.; Knox, J. E.; Hratchian, H. P.; Cross, J. B.; Adamo, C.; Jaramillo, J.; Gomperts, R.; Stratmann, R. E.; Yazyev, O.; Austin, A. J.; Cammi, R.; Pomelli, C.; Ochterski, J. W.; Ayala, P. Y.; Morokuma, K.; Voth, G. A.; Salvador, P.; Dannenberg, J. J.; Zakrzewski, V. G.; Dapprich, S.; Daniels, A. D.; Strain, M. C.; Farkas, O.; Malick, D. K.; Rabuck, A. D.; Raghavachari, K.; Foresman, J. B.; Ortiz, J. V.; Cui, Q.; Baboul, A. G.; Clifford, S.; Cioslowski, J.; Stefanov, B. B.; Liu, G.; Liashenko, A.; Piskorz, P.; Komaromi, I.; Martin, R. L.; Fox, D. J.; Keith, T.; Al-Laham, M. A.; Peng, C. Y.; Nanayakkara, A.; Challacombe, M.; Gill, P. M. W.; Johnson, B.; Chen, W.; Wong, M. W.; Gonzalez, C.; Pople, J. A. Gaussian, Inc., Wallingford CT, 2004.

[82] Medeiros, W. R. Projeção de fármacos: um estudo QSAR de ftalimídas e análogo. [Master's thesis] João Pessoa: Centro das Ciências Exatas e da Natureza, Departamento de Química (DQ) da Universidade Federal da Paraíba, 2004.

[83] Nunes, C. A.; Freitas, M. P.; Pinheiro, A. C. M.; Bastos, S. C. *J. Braz. Chem. Soc.* **2012**, *23*, 2003. **[Crossref]**

[84] **https://www.ufla.br/chemoface,** access January 2021.

[85] Morris, G. M.; Huey, R.; Lindstrom, W.; Sanner, M. F.; Belew, R. K.; Goodsell, D. S.; Olson, A. J. *J. Comput. Chem.* **2009**, *30*, 2785. **[Crossref]**

[86] Trott, O.; Olson, A. J. *J. Comput. Chem.* **2010**, *31*, 455. **[Crossref]**

[87] The PyMOL Molecular Graphics System, Version 2.0 Schrödinger, LLC.

[88] Accelrys Software, Discovery Studio Modeling Environment, Release 4.0, Accelrys Software, San Diego, Calif, USA, 2013.

[89] Pfefferkorn, J. A.; Choi, C.; Larsen, S. D.; Auerbach, B.; Hutchings, R.; Park, W.; Askew, V.; Dillon, L.; Hanselman, J. C.; Lin, Z.; Lu, G. H.; Robertson, A.; Sekerke, C.; Harris, M. S.; Pavlovsky, A.; Bainbridge, G.; Caspers, N.; Kowala, M.; Tait, B. D. *J. Med. Chem.* **2008**, *51*, 31. **[Crossref]**

[90] **Supplementary material: 5.1 Scores and loadings of the PCA**

[91] da Silva, J. B. P.; Ramos, M. N.; Neto, B. B.; de Melo, S. J.; Falcão, E. P. S.; Catanho, M. T. J. A. *J. Braz. Chem. Soc.* **2008**, *19*, 337. **[Crossref]**

[92] Ferreira, M. M. C.; Antunes, A. M.; Melgo, M. S.; Volpe, P. L. O. *Quim. Nova* **1999**, *22*, 1. **[Crossref]**

[93] Ferreira, M. M. C. *J. Braz. Chem. Soc.* **2002**, *13*, 742. **[Crossref]**

[94] **Supplementary material: 5.2 Additional information of the chemometric procedure**

[95] Silla, J. M.; Nunes, C. A.; Cormanich, R. A.; Guerreiro, M. C.; Ramalho, T. C.; Freitas, M. P. *Chemom. Intell. Lab. Syst.* **2011**, 108, 146. **[Crossref]**

[96] Kiralj, R.; Ferreira, M. M. C.; *J. Braz. Chem. Soc.* **2009**, *20*, 770. **[Crossref]**

[97] Finkelmann, A. R.; Göller, A. H.; Schneider, G.; *Chem. Commun.* **2016**, *52*, 681. **[Crossref]**

[98] Fresqui, M. A. C.; Ferreira, M. M. C.; Trsic, M.; *Anal. Chim. Acta*, **2013**, *759*, 43. **[Crossref]**

[99] Desiraju, G. R. *Angew. Chem. Int. Ed.* **2011**, *50*, 52. **[Crossref]**

[100] Oliveira, B. G.; Araújo, R. C. M. U.; Ramos, M. N. *Orbital: Electron. J. Chem.* **2009**, *1*, 156. **[Link]**

[101] Rego, D. G.; Oliveira, B. G. *Orbital: Electron. J. Chem.* **2016**, *8*, 1. **[Crossref]**

[102] Oliveira, B. G. *Orbital: Electron. J. Chem.* **2019**, *11*, 205. **[Crossref]**

[103] Stanley, F. M.; Linder, K. M.; Cardozo, T. J. *PLoS ONE* **2015**, *10*, 1. **[Crossref]**

[104] Tripathi, J.; Mahto, M. K.; Bhaskar, D. R. M.; Shahbazi, S. *Asian J. Res. Chem.* **2012**, *3*, 386. **[Crossref]**

How to cite this article